


# Application of dual-energy computed tomography in preoperative evaluation of Ki-67 expression levels in solid non-small cell lung cancer

Shuangfeng Tian MS<sup>a</sup>, Xia Jianguo MS<sup>b,\*</sup> , Weizhong Tian MS<sup>b</sup>, Yuan Li BS<sup>b</sup>, Jianfeng Hu BS<sup>b,\*</sup>, Mingjun Wang PhD<sup>c</sup>, Juntao Zhang PhD<sup>d</sup>

## Abstract

To investigate whether there were significant differences in dual-energy CT (DECT) in reflecting different quantitative parameters among different levels of Ki-67 expression in patients with solid non-small cell lung cancer (NSCLC). The diagnosis performance of DECT in patients with solid lung adenocarcinoma (LAC) among NSCLC was further discussed. Two hundred fifteen patients confirmed with solid NSCLC were enrolled and analyzed retrospectively in this study. 148 patients were confirmed with LAC among all patients. Three expression levels of Ki-67 were determined by the percentage of Ki-67 positive cancer cells with immunohistochemistry: high-level group (>30%), middle-level group (10%–30%), and low-level group (≤10%). And the latter two levels also known as non-high-level group. The quantitative parameters of enhanced chest DECT (venous phase, VP), including iodine concentration (IC), water concentration (WC), CT value at 40 keV (CT40keV), the slope of energy spectral attenuation curve ( $\lambda_{HU}$ ) and normalized iodine concentration (NIC) were measured and calculated by gemstone spectral imaging Viewer software. One-way ANOVA was used for the comparison of normal distribution DECT parameters between three levels for patients with NSCLC and patients with LAC. Non-normal distribution data were tested by non-parametric test. In addition, the receiver operating characteristic curve of statistically significant DECT parameters was drawn to distinguish the non-high-level and the high-level of Ki-67. Area under the curve (AUC), sensitivity, specificity was calculated to measure the diagnostic performance of parameter. Both in solid NSCLC and LAC, the IC, NIC, WC,  $\lambda_{HU}$  and CT40keV at VP in the high-level group were significantly lower than those in the middle- and low-level group respectively, and the WC at VP in the high-level group was significantly higher than that in the middle- and low-level group respectively (all  $P < .05$ ). Receiver operating characteristic analysis showed that IC and  $\lambda_{HU}$  at VP performed better in distinguishing the high-level and the non-high-level of Ki-67 (NSCLC: AUC = 0.713 and 0.714 respectively; LAC: AUC = 0.705 and 0.706 respectively). Quantitative parameters of DECT provide a new non-invasive method for evaluating the proliferation of cancer cells in solid NSCLC and LAC.

**Abbreviations:**  $\lambda_{HU}$  = the slope of energy spectral attenuation curve, AP = arterial phase, AUC = area under the curve, CT100keVCT = value at 100 keV, CT40keVCT = value at 40 keV, DECT = dual-energy CT, IC = iodine concentration, LAC = lung adenocarcinoma, NIC = normalized iodine concentration, NSCLC = non-small cell lung cancer, ROC = receiver operating characteristic, SCC = squamous cell carcinoma, VP = venous phase, WC = water concentration.

**Keywords:** dual-energy CT, ki-67, solid lung adenocarcinoma, solid non-small cell lung cancer

## 1. Introduction

Lung cancer is one of the most common malignant tumors in the world, which seriously affects human health.<sup>[1]</sup> The American Cancer Society estimates that lung cancer is not only one of the three most common tumors for both men and women in 2019 (the incidence is all about 13%), but also the most common cancer killer in both sexes combined (the mortality rate is about 24% for man and 23% for women).<sup>[2]</sup>

Approximately up to 85% of lung cancers are classified as non-small cell lung cancer (NSCLC), which the mortality rate is high.<sup>[3]</sup> Despite remarkable progress has been made in the diagnosis and treatment of lung cancer in recent years, the prognosis is still poor, with a 5-year survival rate of less than 16%. And even if patients diagnosed with stage I, the 5-year survival rate is less than 70%.<sup>[4,5]</sup> There is thus an urgent need to find some reliable prognostic factors to predict the clinical outcome of patients with lung cancer.

This research was supported by the Taizhou People's Hospital (ZL202016) awarded to Jianguo Xia.

Institutional Review Board approval was obtained.

The authors have no conflicts of interest to disclose.

The datasets generated during and/or analyzed during the current study are available from the corresponding author on reasonable request.

<sup>a</sup>Graduate School of Dalian Medical University, Dalian, PR China, <sup>b</sup>Department of Radiology, Taizhou People's Hospital, Taizhou, PR China, <sup>c</sup>CT Research Centre GE China, Shanghai, PR China, <sup>d</sup>GE Healthcare, Precision Health Institution, Shanghai, PR China.

\*Correspondence: Jianguo Xia, Department of Radiology, Taizhou People's Hospital, No. 366 Taihu Road, Yiyaoqiaoxin District, Taizhou, Jiangsu 225300, PR China (e-mail: shjxct@163.com).

Copyright © 2022 the Author(s). Published by Wolters Kluwer Health, Inc.

This is an open-access article distributed under the terms of the Creative Commons Attribution-Non Commercial License 4.0 (CCBY-NC), where it is permissible to download, share, remix, transform, and buildup the work provided it is properly cited. The work cannot be used commercially without permission from the journal.

How to cite this article: Tian S, Jianguo X, Tian W, Li Y, Hu J, Wang M, Zhang J. Application of dual-energy computed tomography in preoperative evaluation of Ki-67 expression levels in solid non-small cell lung cancer. *Medicine*. 2022;101:31(e29444).

Received: 25 November 2021 / Received in final form: 22 April 2022 / Accepted: 22 April 2022

<http://dx.doi.org/10.1097/MD.000000000029444>

At present, some biomarker predictors, such as Ki-67, have shown important clinical value in the treatment and prognosis of patients with lung cancer.<sup>[6]</sup> Ki-67 is a DNA-binding nuclear protein, its expression level increases rapidly from G1 to mitotic stage, and then decreases rapidly, but does not exist in quiescent cells (G0 phase), so Ki-67 is used to distinguish between growing and non-growing cells.<sup>[7,8]</sup> A large number of meta-analyses showed that the high-level of Ki-67 was associated with poor prognosis after resection of lung tumor,<sup>[9]</sup> short tumor-free survival<sup>[5,10]</sup> and short recurrence-free survival.<sup>[11]</sup> Immunohistochemical (IHC) examination is usually a routine method to detect the expression of Ki-67, but it requires invasive methods such as biopsy using percutaneous needle biopsy or bronchoscopy to obtain specimens, which may lead to bleeding or pneumothorax<sup>[12]</sup> and increase the chance of tumor metastasis. In addition, due to the heterogeneity in the tumor and the small sample size in individual cases, biopsies may miss more invasive lesions in the tumor and underestimate the invasive ability of cancer cells. Therefore, an accurate and non-invasive method is clinically demanded to predict the expression of Ki-67 in patients with NSCLC.

Recently, tissue can be quantitatively and qualitatively analyzed by dual-energy CT (DECT) imaging, which opens up a new field for CT imaging.<sup>[13]</sup> DECT imaging technology obtains dual-energy imaging data through fast switching between low and high voltage (80/140 kVp).<sup>[6,14,15]</sup> It can reconstruct monochromatic images of 40 to 140 keV and quantitatively measure iodine concentration (IC) and water concentration (WC) by material decomposition images to reflecting tumor blood flow. In addition, it can also reflect the structural differences of tumors by changing with the attenuation of photon energy (energy spectral attenuation curve).<sup>[6,13-15]</sup> DECT imaging may be of great value in the preoperative evaluation the expression level of Ki-67 in NSCLC.

The purpose of this study was to explore whether there were significant differences in quantitative parameters of DECT among different levels of Ki-67 expression in patients with solid NSCLC and lung adenocarcinoma (LAC).

## 2. Methods

### 2.1. Study population

Our institutional review board (Taizhou People's Hospital, China) approved this retrospective cohort study. And our retrospective study was performed with a waiver of written informed consent. Retrospective review of a database at our institution identified 1333 consecutive patients who confirmed with primary lung cancer by surgical resection or biopsy, from July 2018 to December 2020. Clinical data of all cases were collected. According to the inclusion and exclusion criteria, the patient recruitment path way is showed in Figure 1.

The inclusion criteria were as follows: (1) chest CT enhanced scan adopts gemstone spectral imaging (GSI) mode of revolution CT (GE Healthcare, WI, Milwaukee, USA) before surgery or biopsy; (2) image quality was acceptable; (3) chest CT imaging showed solid nodules and masses with a maximum diameter of >10mm in the lung window; (4) LAC and squamous cell carcinoma (SCC) were confirmed by histopathology, and the expressi-4 on percentage of Ki-67 positive cancer cells was determined by IHC examination. The exclusion criteria were as follows: (1) have a history of cancer other than lung cancer; (2) after the treatment of lung cancer.

A total of 215 patients were finally included (male 134, female 81). The age range was 42 to 87 years old, and the average age was  $66.85 \pm 8.79$  years old.

### 2.2. Dual-energy CT imaging

Patients underwent enhanced chest CT examination with GSI mode on a revolution CT (GE Healthcare) before surgery or

biopsy. Scanning parameters were as follows: The low and high tube voltage 80/140 rapid-kVp-switch; the tube current was 405 mA; rotation speed 0.5 s/cr; the pitch was 0.992; the layer thickness was 5 mm; the layer spacing was 5 mm; and. The images of 1.25 mm layer thickness and layer spacing were also reconstructed automatically. A total of 80 mL of non-ionic iodinated contrast medium (Iohexol Injection, 300 mgI/L; Yangtze River Pharmaceutical, Jiangsu, China) was injected intravenously at the rate of 2.5 mL/s. The Smart Phase threshold trigger technique was used. After the injection, the arterial phase (AP) scan was started when the threshold of the descending aorta reached 120 HU, and then the venous phase (VP) scan was delayed for 20 seconds after AP.

### 2.3. Image analysis

The original images of 1.25 mm slice thickness in VP were reconstructed and transferred to an advanced workstation (ADW4.7; GE Healthcare) for analysis. Combining with the pathological results, three consecutive image sections containing the maximum cross-section of the uniform solid part of the lesion and the upper and lower levels were selected to outline the region of interests (ROIs). ROIs were drawn as big as possible to cover most part of the mass region, avoiding areas with cystic degeneration, necrosis, blood vessels and calcification. And the paste-and-copy function was applied to make a sure that the position, size and shape of ROIs on the monochromatic image sets, iodine- and water-based material decomposition images were consistent. All ROIs were drawn by the two radiologists with both have 3-year experience in chest CT through consultation. In case of the two physicians did not agree on the ROI, a third radiologist with over 20-year experience in chest CT would assess and make a final conclusion. The CT values of 40 keV and 100 keV (CT40keV and CT100keV) were measured from the monochromatic images of 40 keV and 100 keV in the VP, and IC and WC were measured from the iodine- and water-based materials decomposition images. After continuous measurement of three levels, the average value is calculated to reduce the measurement deviation.

In order to minimize the effect of individual variation (such as circulation status and scanning times), the normalised iodine concentration (NIC) was calculated as following formula:  $NIC = IC_{lesion}/IC_{artery}$ . And the spectral attenuation curves were automatically generated by plotting the material attenuation against x-ray photon energy with GSI Viewer software by propagating the ROIs to all virtual monochromatic image sets with energies from 40 to 140 keV. Then the slope of the spectral attenuation curve ( $\lambda_{HU}$ ) which range from 40 keV to 100 keV was calculated by the following formula:  $\lambda_{HU} = (CT40keV - CT100keV)/60$ .

### 2.4. Ki-67 assessment

Four-micron-thick sequential sections were used for IHC. And ready-to-use monoclonal mouse anti-human Ki-67 antibody (Dako, DK-2600, Glostrup, Denmark) was used for IHC examination. The antigen-antibody reaction experiment was carried out according to the instructions of the kit. Cells with brown nuclei were considered to be positive cells. After investigating the whole specimen, five regions with the highest expression of Ki-67 were selected. 100 cells in each region were randomly counted under 400× magnification, and Ki-67 expression was defined as the percent of Ki-67 positive cancer cells divided by the total number of cancer cells within one high power field. The Ki-67 values were calculated in the five regions and then averaged.

According to previous studies,<sup>[6,16,17]</sup> the Ki-67 value was divided into three levels: the Ki-67 value >30% was divided into the high-level, 10% to 30% into the middle-level, and ≤10% into the low-level. The middle-level and the low-level also known as the non-high-level.

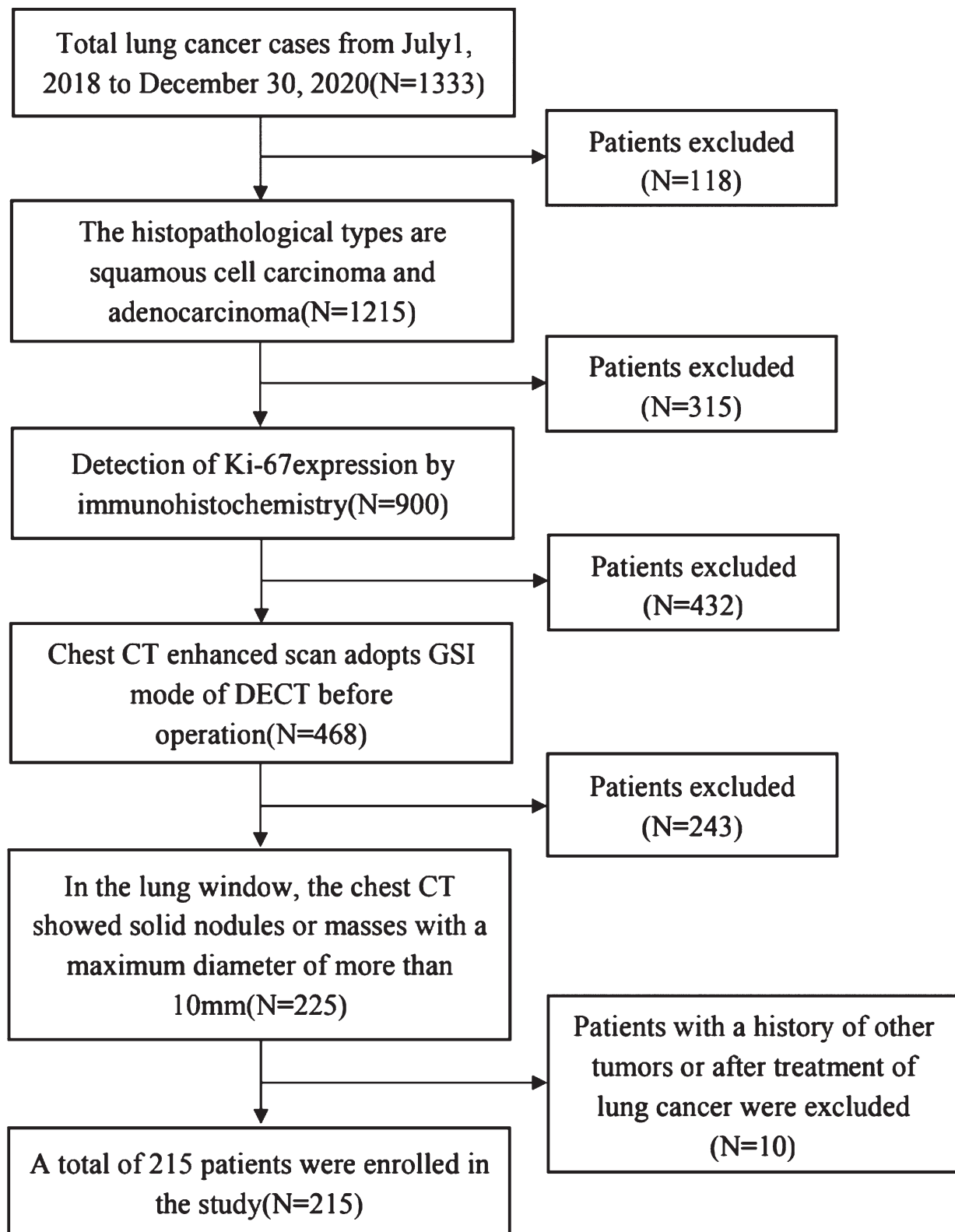


**Figure 1.** Schematic flow chart of patient inclusion and exclusion criteria.

### 2.5. Statistical analysis

The quantitative parameters of DECT were performed using SPSS (version 20.0.0; IBM, Armonk, NY, USA) statistical software, and the graphing software used was GraphPad Prism (version 8.3.0; San Diego, CA, USA). All *P* values were bilateral, and *P* < .05 was considered to be statistically significant.

The data was assessed by test of normality. Data with the normal distribution and uniform variance was expressed by mean  $\pm$  standard deviation ( $\pm x \pm s$ ), otherwise it was expressed by the median (first quartile, third quartile). One-way ANOVA was used for comparison between multiple groups of data conforming to normal distribution and uniform variance, then LSD-*t*

pairwise comparison was used to further analyze the differences of quantitative parameters within the group. For data sets with non-normal distributed or uneven variances, a Kruskal–Wallis test was used. When the result of the Kruskal–Wallis test indicated a significant difference, Post-hoc tests were made using multiple pairwise comparisons with the Bonferroni correction for Kruskal–Wallis test.

In addition, the receiver operating characteristic (ROC) curves with statistically different energy spectral parameters were drawn. The optimal cut-off values of energy spectral parameters to distinguish the high-level from the non-high-level of Ki-67 were determined using ROC analysis. And the differential diagnosis performance of each parameter was measured by the area under the curve (AUC). The sensitivity and specificity for each parameter in distinguishing the level of Ki-67 expression were calculated using the optimal cut-off values determined by the ROC curves.

### 3. Results

#### 3.1. Patient information

Among the total 215 patients with solid NSCLC (148 LAC, 67 SCC) who received surgery or biopsy after DECT examination were enrolled. The clinical characteristics of the 215 patients are summarized in Table 1. According to the grouping standard, there were 94 patients with the high-level of Ki-67 expression (48 LAC, 46 SCC), 71 patients with the middle-level (55 LAC, 16 SCC), and 50 patients with the low-level (45 LAC and 5 SCC). Images of DECT at VP is shown in Figures 2–4.

#### 3.2. Comparison of energy spectral parameters

There were significant differences in IC, NIC, WC,  $\lambda_{\text{HU}}$  and CT40keV at VP among the high-, middle- and low-level Ki-67 expression groups of solid NSCLC (IC, CT40keV and  $\lambda_{\text{HU}}$ : one-way ANOVA,  $P < .05$ ; NIC, WC: Kruskal–Wallis test,  $P < .05$ ). And IC, NIC,  $\lambda_{\text{HU}}$  and CT40keV at VP in the high-level were significantly lower than those in the middle and low-level, respectively ( $P < .05$ ). In addition, WC at VP in the high-level was significantly higher than that in the middle- and low-level ( $P < .05$ ). But there was no significant difference in all energy spectral parameters between the low-level and the middle-level ( $P > .05$ ). Details as shown in Table 2.

IC, NIC, WC, K and CT40keV at VP were significantly different among the high-, middle- and low-level Ki-67 expression of solid LAC (IC, NIC, CT40keV and K: One-way ANOVA,  $P < .05$ ; WC: Kruskal–Wallis test,  $P < .05$ ). And IC, NIC, WC,  $\lambda_{\text{HU}}$  and CT40keV at VP of the high-level were significantly lower than those of the middle- and low-level respectively ( $P < .05$ ). In addition, WC at VP of the high-level was significantly higher than that of the middle- and low-level ( $P < .05$ ). But there was no significant difference in all energy spectral parameters between the low-level and the middle-level ( $P > .05$ ). Details as shown in Table 3.

**Table 1**  
Summary of patient clinical characteristics.

Characteristic	
Age (y), mean and range	66.18 ± 8.61
Sex	
Male	134 (62.33%)
Female	81 (37.67%)
Pathologic types	
Adenocarcinoma	148 (68.84%)
Squamous cell carcinoma	67 (31.16%)

#### 3.3. ROC curve analysis

According to the above analysis, there were statistical differences in IC, NIC, WC,  $\lambda_{\text{HU}}$  and CT40keV at VP between the high-level and the middle- and low-level respectively both in solid NSCLC and LAC. There was no significant difference in all quantitative parameters between the middle-level and the low-level both in solid NSCLC and LAC. Therefore, the main purpose of this study was to analyze the effectiveness of IC, NIC, WC,  $\lambda_{\text{HU}}$  and CT40<sub>keV</sub> at VP in distinguishing the high-level Ki-67 from the non-high-level both in solid NSCLC and LAC.

In solid NSCLC, The ROC analysis showed that IC and  $\lambda_{\text{HU}}$  performed the best in distinguishing the high-level and the non-high-level (AUC = 0.713 and 0.714 respectively). And the sensitivity and specificity of IC and  $\lambda_{\text{HU}}$  were as follows: for IC, 64.5% and 72.3% with cut-off value of 22.845; for  $\lambda_{\text{HU}}$ , 65.3% and 72.3% with cut-off value of 2.705. Details as shown in Table 4 and Figure 5.

And in solid LAC, the ROC analysis also demonstrated that IC and  $\lambda_{\text{HU}}$  performed the best in distinguishing the high-level and the non-high-level (AUC = 0.705 and 0.706 respectively). And the sensitivity and specificity of IC and  $\lambda_{\text{HU}}$  were as follows: for IC, 72% and 66.7% with cut-off value of 22.845; for  $\lambda_{\text{HU}}$ , 73% and 66.7% with cut-off value of 2.705. Details as shown in Table 4 and Figure 5.

### 4. Discussion

In this study, we analyzed whether there were significant differences in quantitative parameters of DECT among different Ki-67 expression groups in solid NSCLC and LAC, so as to find out that the optimal cut-off value could be used as a non-invasive predictor of the Ki-67 expression in patients with solid NSCLC and LAC. The results showed that there were significant differences in spectral parameters (including IC, NIC, WC, CT40keV,  $\lambda_{\text{HU}}$  in VP) between the high-level group and the middle- and low-level group of Ki-67 in solid NSCLC, and the diagnostic efficiency of  $\lambda_{\text{HU}}$  in VP was best (AUC = 0.714). When the optimal cut-off value of K was 2.705, the sensitivity, specificity of diagnosing Ki-67 high expression was 65.3% and 72.3% respectively. In addition, in the subgrouping according to the pathological type, there were also statistically significant difference in the spectral parameters between the high-level group and the middle- and low-level group of Ki-67 in solid LAC. And the ROC analysis that 2.705 of  $\lambda_{\text{HU}}$  in VP was the optimal cut-off value to discriminate the expression of Ki-67 and yielded the following: for  $\lambda_{\text{HU}}$  in VP, sensitivity of 73%, specificity of 66.7%, with an AUC of 0.706. The find indicates that the quantitative parameters of DECT may have a role in predicting the proliferation of solid NSCLC and LAC before operation.

Lung cancer is the leading cause of cancer-related deaths. The proliferative activity of lung cancer has a significant effect on its growth, invasion, metastatic potential and sensitivity to radiotherapy and chemotherapy. Therefore, evaluating the proliferative activity of tumor tissue plays a key role in predicting the overall prognosis and treatment response of patients with NSCLC. Ki-67 is a reliable marker for identifying proliferating cells in human and animal tumors, and its expression is related to the growth fraction of cancer cells.<sup>[15]</sup> In the past, some researchers used MSCT,<sup>[18]</sup> MRI,<sup>[19]</sup> and PET-CT<sup>[20]</sup> to study the expression level of Ki-67 in NSCLC or LAC, however, these imaging methods of these studies were either single or complex and expensive. The fast switching technology of single tube is used in DECT imaging, which can realize the fast switching of high and low energy (140 kVp and 80 kVp) in the process of rotation. Energy spectral imaging can generate 101groups of 40 to 140 keV monochromatic images, optimize the image quality and improve the image contrast. It can also generate iodine decomposition images reflecting tumor blood flow and energy spectral attenuation curves reflecting different chemical composition and

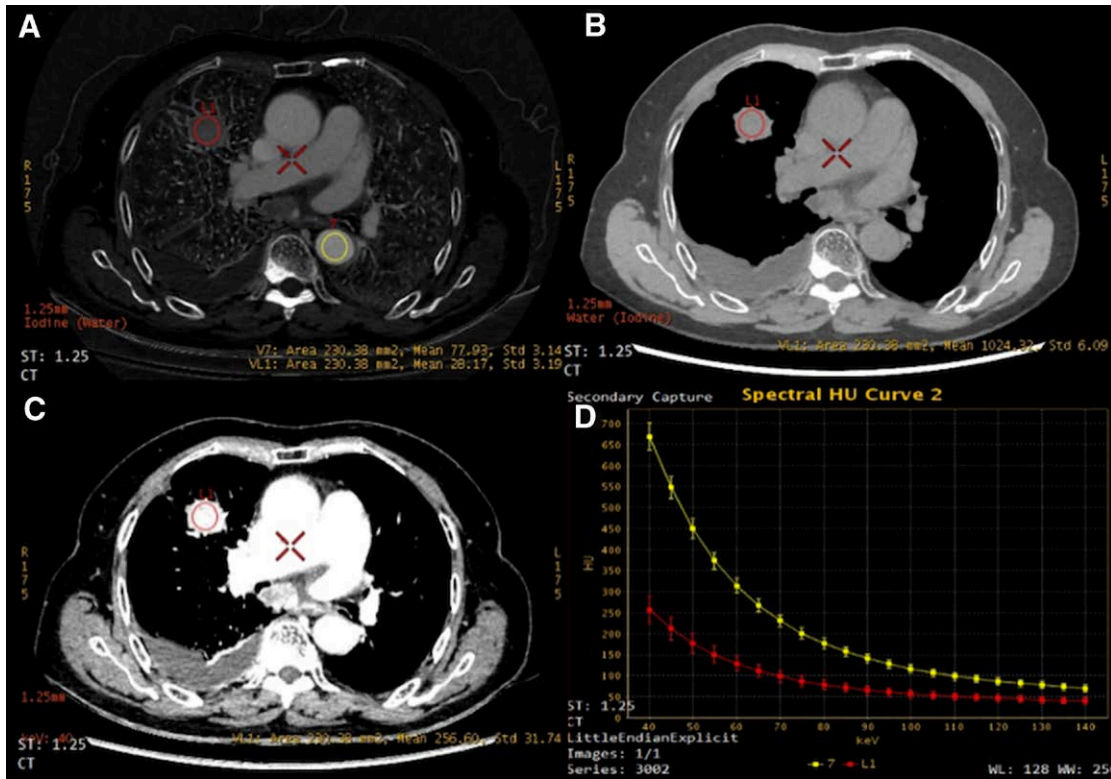


**Figure 2.** A 70-year-old female with right upper lung adenocarcinoma, Ki-67 = 5%. (A) The iodine-based materials decomposition image, IC = 28.17 (mg/ml). (B) The water-based materials decomposition image, WC = 1024.32 (mg/cm<sup>3</sup>). (C) The single energy image of CT value at 40 keV, CT40keV = 256.60HU. (D) The spectral attenuation curve,  $\lambda_{HU}$  = 3.33.

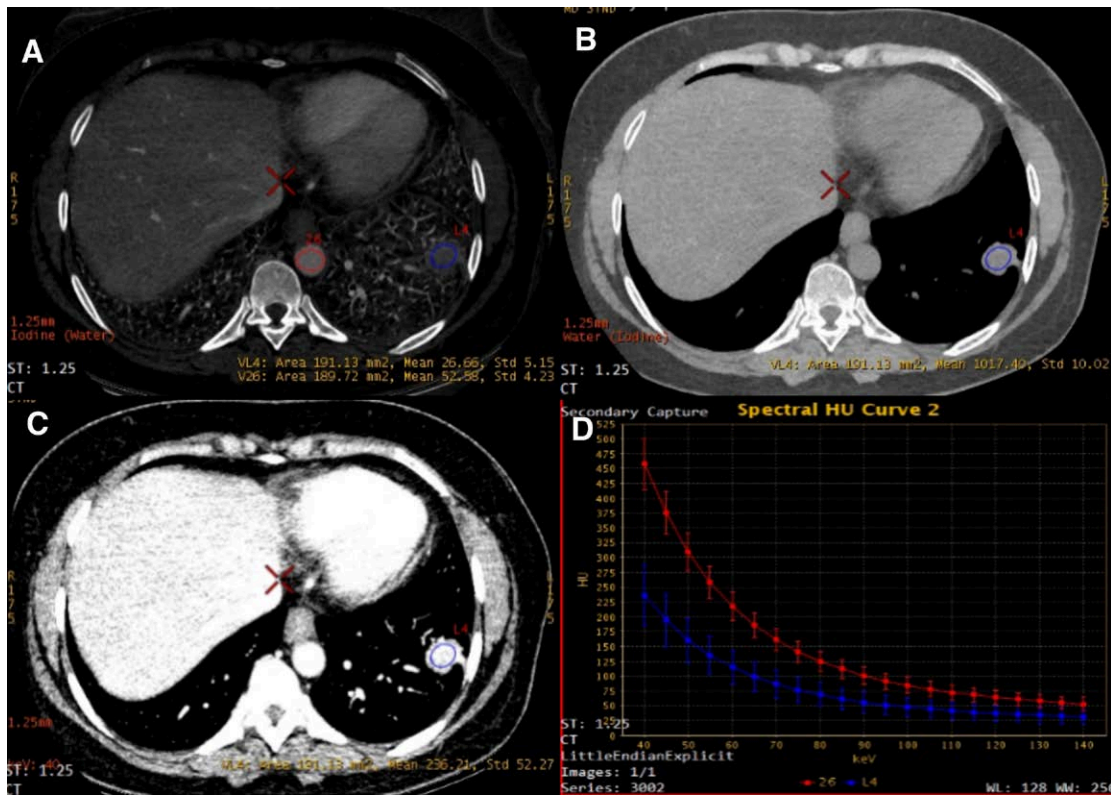


**Figure 3.** A 49-year-old female with left lower lung adenocarcinoma, Ki-67 = 30%. (A) The iodine-based materials decomposition image IC = 26.66 (mg/ml). (B) The water-based materials decomposition image, WC = 1017.40 (mg/cm<sup>3</sup>). (C) The single energy image of CT value at 40 keV CT40keV = 236.21HU. (D) The spectral attenuation curve,  $\lambda_{HU}$  = 3.14.

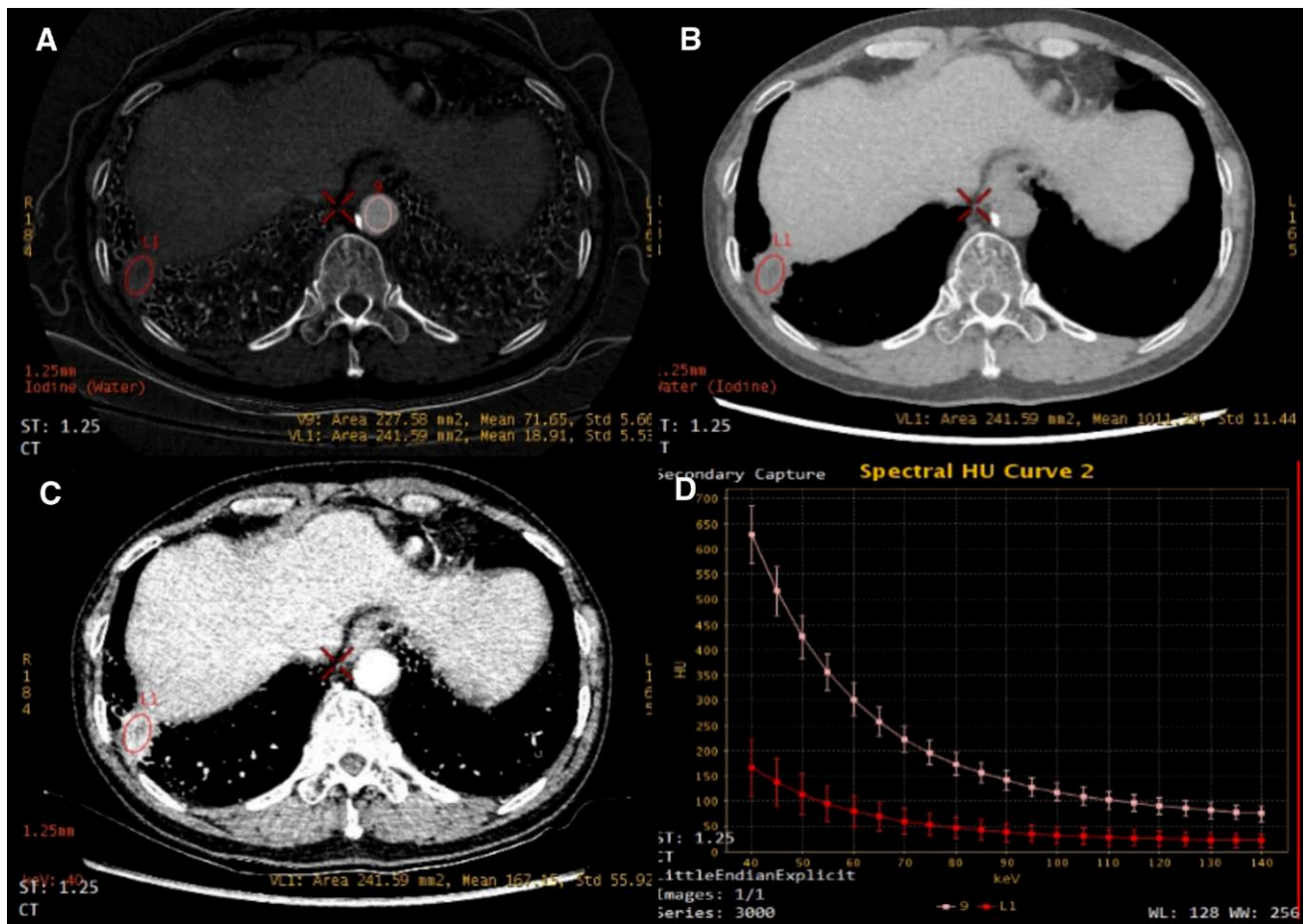


**Figure 4.** A 71-year-old male with right lower lung Squamous cell carcinoma, Ki-67 = 70%. (A) The iodine-based materials decomposition image, IC = 18.91 (mg/ml). (B) The water-based materials decomposition image, WC = 1011.29 (mg/cm<sup>3</sup>). (C) The single energy image of CT value at 40 keV, CT40keV = 167.15HU. (D) The spectral attenuation curve,  $\lambda_{HU} = 2.24$ .

material structure, and carry out multi-parameter quantitative analysis.<sup>[21,22]</sup> It is helpful to evaluate the biological behavior of NSCLC.

Enhanced CT values, IC and NIC can reflect the blood perfusion of tumor to some extent, and WC can reflect the water content of intracellular and extracellular tissue.<sup>[6,13,23]</sup> It has been reported<sup>[24]</sup> that during the arterial period, the contrast medium can't completely fill the micro-vessels in a short time. However, during the VP, there is a longer delay after contrast injection than in the AP, allowing the contrast medium to well fill the micro-vessels and penetrate the basement membrane into the

intercellular space. Therefore, IC in VP can more effectively reflect the blood flow distribution of lung cancer. Therefore, VP was selected as the research phase in this study.

In the past study, Lin et al<sup>[6]</sup> found that IC and NIC in arteriovenous phase of the high-level Ki-67 expression group was significantly lower than the low-level Ki-67 expression group in NSCLC ( $P < .001$ ). However, Chen et al<sup>[16]</sup> reported that there was no significant difference in IC and NIC in arteriovenous phase among the four grades of Ki-67 labeling index in LCA, and there was moderate positive correlation between CT40keV and Ki-67 labeling index in arteriovenous phase of LAC. But

**Table 2**

**Comparison of different expression levels of Ki-67 in solid non-small cell lung cancer.**

Group	N	IC	NIC	WC	CT40keV	$\lambda_{HU}$
Low-level	50	25.86 ± 7.13* <sup>‡</sup>	0.43 (0.56, 0.3)* <sup>‡</sup>	1016.29 (1024.37, 998.52)* <sup>‡</sup>	224.09 ± 53.47* <sup>‡</sup>	3.06 ± 0.84* <sup>‡</sup>
Middle-level	71	24.25 ± 6.91*	0.41 (0.53, 0.31)*	1018.07 (1023.89, 1010.72)*	216.75 ± 51.72*	2.87 ± 0.82*
High-level	94	19.86 ± 5.49	0.36 (0.27, 0.43)	1022.32 (1029.96, 1017.55)	186.05 ± 42.72	2.35 ± 0.66
<i>F</i> / <i>χ</i> <sup>2</sup>		17.52	13.75	18.52	13.17	17.61
<i>P</i>		<.05	<.001	<.001	<.05	<.05

IC, CT40keV  $\lambda_{HU}$  satisfies normal distribution and uniform variance. The difference of IC, CT40keV and  $\lambda_{HU}$  among three groups was tested by one-way ANOVA, and LSD-*t* was used to compare the differences between two groups. NIC satisfies normal distribution, but the variance is uneven, and WC does not satisfy normal distribution. The difference of NIC and WC among three groups was tested by Kruskal-Wallis test. Post-hoc tests were made using multiple pairwise comparisons. Differences were considered significant at  $P < .05$  (two-sided).

$\lambda_{HU}$  = slope of the spectral attenuation curve (40–100 keV), CT40keV = CT value at 40 keV, IC = iodine concentration, N = number of patients, NIC = normalized iodine concentration, WC = water concentration.

\*Compared with the high level ( $P < .05$ ).

‡Compared with the medium level ( $P > .05$ ).

**Table 3**  
**Comparison of different expression levels of Ki-67 in solid lung adenocarcinoma.**

Group	N	IC	NIC	WC	CT40keV	$\lambda_{HU}$
Low-level	45	26.09 ± 7.33*,†	0.44 ± 0.17*,†	1015.07 (1020.94, 997.94)*,†	224.22 ± 55*,†	3.09 ± 0.87*,†
Middle-level	55	25.90 ± 6.50*	0.46 ± 0.15*	1016.54 (1023.5, 1008.53)*	228.72 ± 48.35*	3.07 ± 0.77*
High-level	48	21.04 ± 6.19	0.36 ± 0.13	1021.45 (1016.39, 1028.01)	194.88 ± 48.76	2.49 ± 0.74
F/x2		8.92	6.17	15.03	6.51	8.93
P						

IC, NIC, CT40keV,  $\lambda_{HU}$  satisfies normal distribution and uniform variance. The difference of IC, NIC, CT40keV and  $\lambda_{HU}$  among three groups was tested by one-way ANOVA, and LSD-t was used to compare the differences between two groups. WC does not satisfy normal distribution. The difference of WC among three groups was tested by Kruskal–Wallis test. Post-hoc tests were made using multiple pairwise comparisons. Differences were considered significant at  $P < .05$  (two-sided).

$\lambda_{HU}$  = slope of the spectral attenuation curve (40–100 keV), CT40keV = CT value at 40 keV, IC = iodine concentration, N = number of patients, NIC = normalized iodine concentration, WC = water concentration.

\*Compared with the high-level ( $P < .05$ ).

†Compared with the medium level ( $P > .05$ ).

**Table 4**  
**Performance of differential parameters in distinguishing the high-level and the non-high level of Ki-67.**

Parameter	Non-small cell lung cancer					Lung adenocarcinoma				
	IC	NIC	WC	CT40keV	$\lambda_{HU}$	IC	NIC	WC	CT40keV	$\lambda_{HU}$
AUC	0.713	0.646	0.663	0.684	0.714	0.705	0.669	0.686	0.665	0.706
Sensitivity	64.5%	47.1%	25%	71.9%	65.3%	72%	53%	3%	78%	73%
Specificity	72.3%	85.1%	100%	61.7%	72.3%	66.7%	81.2%	100%	50%	66.7%
Youden index	0.368	0.322	0.025	0.336	0.376	0.387	0.342	0.003	0.280	0.397
Cut-off value	22.845	0.444	1041.730	196.423	2.705	22.845	0.442	1040.198	194.042	2.705

$\lambda_{HU}$  = slope of the spectral attenuation curve (40–100 keV), AUC = area under the curve, CT40keV = CT value at 40 keV, IC = iodine concentration, NIC = normalized iodine concentration, WC = water concentration.

we found whether it's solid NSCLC or LAC in present study, the value of IC, NIC, CT40keV at VP of the high-level group were lower than those of the middle-level group and the low-level group, but there was no significant difference between the middle-level group and the low-level group. This study is contrary to the traditional view. Fan et al<sup>[15,25]</sup> found that the level of Ki-67 expression was correlated positively with the value of NIC and IC in gastric cancer and rectal cancer. They thought that the higher the tumor Ki-67 is, the more active the tumor proliferation and growth is, the more abundant the blood supply is, and the higher the IC and NIC is. The reason may be that the NSCLC and LAC with high level of Ki-67 expression has stronger proliferative ability is, larger tumor volume is, higher cell density and relatively insufficient blood perfusion, which leads to the decrease of IC, NIC and CT40keV, the increases of WC.

In addition, Lin et al<sup>[6]</sup> reported that the  $\lambda_{HU}$  (40 to 100 keV range) in arteriovenous phase of the high-level Ki-67 expression group was significantly lower than that of the low-level Ki-67 expression group. However, Chen et al<sup>[16]</sup> reported that there was no significant difference in  $\lambda_{HU}$  (40–70 keV range) among the four grades of LAC in arteriovenous phase. In spectral CT technology, because different chemical composition and tissue structure have different spectral curves, the slope of spectral curves can distinguish different substances.<sup>[13]</sup> Our results showed that  $\lambda_{HU}$  in VP of the high-level group was lower than that of the middle- and low-level group both in LAC and NSCLC, but there was no difference between the middle-level group and the low-level group. These differences can be explained by the fact that tumors with different levels of Ki-67 expression may have different components and tissue structures. The higher the expression level of Ki-67 in tumor, the greater the internal cell density, the

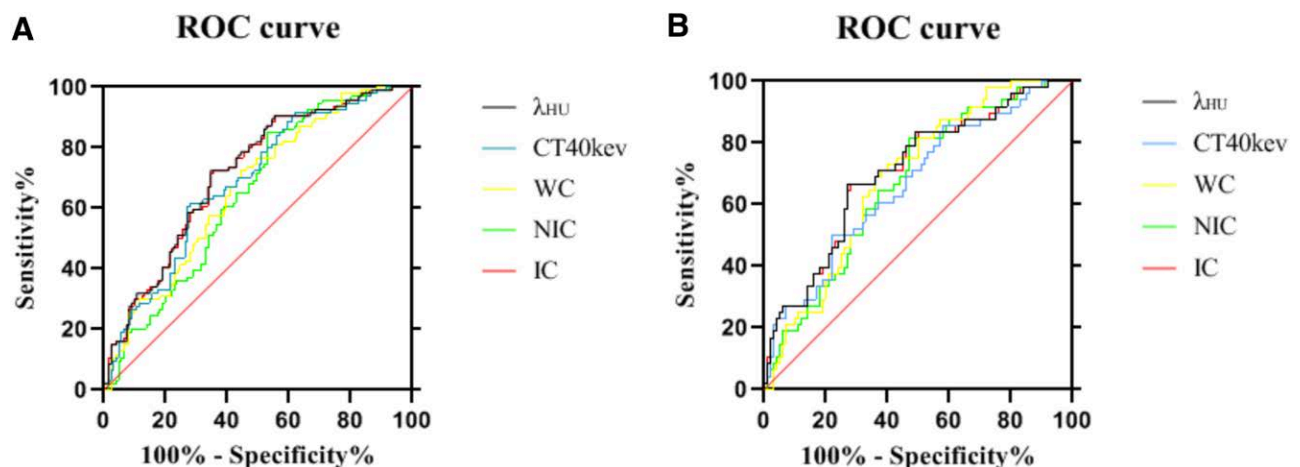


**Figure 5.** ROC curves of spectral parameters used to distinguish the high-level group from the non-high-level group in non-small cell lung cancer (A) and lung adenocarcinoma (B) respectively.

larger the nuclear and cytoplasmic content, the higher the content of macromolecular protein, and the smaller the extracellular space.<sup>[6]</sup>  $\lambda_{HU}$  in VP of NSCLC and LAC reflects the complex chemical composition and tissue structure of the tumor with high proliferative ability. Karaman et al<sup>[19]</sup> reported that there was a significant negative correlation between the minimum apparent diffusion coefficient ( $ADC_{min}$ ) of MRI and the Ki-67 proliferation index of NSCLC ( $r = -0.837, P < .001$ ). Since the ADC value is usually used to quantify the diffusion of water molecules in tissues, this result may suggest that the expression of Ki-67 may affect the internal structure of the tumor, resulting in limited diffusion of water molecules in tissues.

Our research has some limitations. First of all, in order to ensure the accuracy of ROI placement in masses or nodules, tumors with a maximum diameter smaller than 10 mm and ground glass nodules on CT were excluded, so there may be a selection bias. Secondly, because of the heterogeneity of the tumor, although ROI includes the solid components of the lesions as much as possible, we only choose to measure the solid components of the lesions on three levels, not including the whole solid components of the mass, so ROI may not represent the whole tumor. Third, due to the small number of cases of SCC, we did not analyze whether there were differences in energy spectral parameters among different Ki-67 expression levels of SCC.

## 5. Conclusions

In conclusion, there are differences in energy spectral parameters between the high-level group and non-high-level group of Ki-67 of NSCLC and LAC. In the clinical context, these findings will help to non-invasively evaluate the proliferation of NSCLC and LAC before treatment, and provide some value for clinicians to determine treatment options and evaluate the prognosis of patients to improve patient management.

## Acknowledgments

The authors would like to thank the people who participated in this study.

## Author contributions

Data curation: Shuangfeng Tian and Jianfeng Hu.  
 Formal analysis: Weizhong Tian, Yuan Li, and Juntao Zhang.  
 Resources: Jianguo Xia.  
 Writing – original draft: Shuangfeng Tian and Mingjun Wang.  
 Data curation: Jianfeng Hu, Shuangfeng Tian, Yuan Li  
 Formal analysis: Juntao Zhang, Weizhong Tian, Yuan Li  
 Funding acquisition: Jianguo Xia  
 Project administration: Jianguo Xia  
 Resources: Jianguo Xia  
 Writing – original draft: Shuangfeng Tian  
 Writing – review & editing: Mingjun Wang

## References

- Bray F, Ferlay J, Soerjomataram I, et al. Global cancer statistics 2018: Globocan estimates of incidence and mortality worldwide for 36 cancers in 185 countries. *CA Cancer J Clin* 2018;68:394–424.
- Siegel RL, Miller KD, Jemal A. Cancer statistics, 2019. *CA Cancer J Clin* 2019;69:7–34.
- Majem M, Juan O, Insa A, et al. Seom clinical guidelines for the treatment of non-small cell lung cancer (2018). *Clin Transl Oncol* 2019;21:3–17.
- Wang X, Liu H, Shen K, et al. Long intergenic noncoding RNA 00467 promotes lung adenocarcinoma proliferation, migration and invasion by binding with EZH2 and repressing HTRA3 expression. *Mol Med Rep* 2019;20:640–54.
- Wen S, Zhou W, Li CM, et al. Ki-67 as a prognostic marker in early-stage non-small cell lung cancer in Asian patients: a meta-analysis of published studies involving 32 studies. *BMC Cancer* 2015;15:520.
- Lin L, Cheng J, Tang D, et al. The associations among quantitative spectral CT parameters Ki-67 expression levels and EGFR mutation status in NSCLC. *Sci Rep* 2020;10:3436.
- Seigneurin D, Guillaud P. Ki-67 antigen, a cell cycle and tumor growth marker. *Pathol Biol (Paris)* 1991;39:1020–8.
- Gerdes J, Schwab U, Lemke H, et al. Production of a mouse monoclonal antibody reactive with a human nuclear antigen associated with cell proliferation. *Int J Cancer* 1983;31:13–20.
- Martin B, Paesmans M, Mascaux C, et al. Ki-67 expression and patients survival in lung cancer: systematic review of the literature with meta-analysis. *Br J Cancer* 2004;91:2018–25.
- Yamashita S, Moroga T, Tokuiishi K, et al. Ki-67 labeling index is associated with recurrence after segmentectomy under video-assisted thoracoscopic surgery in stage I non-small cell lung cancer. *Ann Thorac Cardiovasc Surg* 2011;17:341–6.
- Sofocleous CT, Garg SK, Cohen P, et al. Ki-67 is an independent predictive biomarker of cancer specific and local recurrence-free survival after lung tumor ablation. *Ann Surg Oncol* 2013;20:S676–83.
- Yao X, Gomes MM, Tsao MS, et al. Fine-needle aspiration biopsy versus core-needle biopsy in diagnosing lung cancer: a systematic review. *Curr Oncol* 2012;19:e16–27.
- Yang L, Luo D, Yi J, et al. Therapy effects of advanced hypopharyngeal and laryngeal squamous cell carcinoma: evaluated using dual-energy CT quantitative parameters. *Sci Rep* 2018;8:9064.
- Li M, Zhang L, Tang W, et al. Quantitative features of dual-energy spectral computed tomography for solid lung adenocarcinoma with EGFR and KRAS mutations, and ALK rearrangement: a preliminary study. *Transl Lung Cancer Res* 2019;8:401–12.
- Fan S, Li X, Zheng L, et al. Correlations between the iodine concentrations from dual energy computed tomography and molecular markers Ki-67 and HIF-1 $\alpha$  in rectal cancer: a preliminary study. *Eur J Radiol* 2017;96:109–14.
- Chen M, Li X, Wei Y, et al. Spectral CT imaging parameters and Ki-67 labeling index in lung adenocarcinoma. *Chin J Cancer Res* 2020;32:96–104.
- Jakobsen JN, Sorensen JB. Clinical impact of Ki-67 labeling index in non-small cell lung cancer. *Lung Cancer* 2013;79:1–7.
- Yan J, Wang H, Zhou H, et al. Correlation between expression of Ki-67 and MSCT signs in different types of lung adenocarcinoma. *Medicine (Baltimore)* 2020;99:e18678.
- Karaman A, Durur-Subasi I, Alper F, et al. Correlation of diffusion MRI with the Ki-67 index in non-small cell lung cancer. *Radiol Oncol* 2015;49:250–5.
- Palumbo B, Capozzi R, Bianconi F, et al. Classification model to estimate MIB-1 (Ki 67) proliferation index in NSCLC patients evaluated with (18)F-FDG-PET/CT. *Anticancer Res* 2020;40:3355–60.
- Zhang Y, Cheng J, Hua X, et al. Can spectral CT imaging improve the differentiation between malignant and benign solitary pulmonary nodules? *PLoS one* 2016;11:e0147537.
- Li M, Zheng X, Gao F, Xiao L, Hua Y. Spectral CT imaging of intranodular hemorrhage in cases with challenging benign thyroid nodules. *Radiol Med* 2016;121:279–90.
- Jia Y, Xiao X, Sun Q, et al. CT spectral parameters and serum tumour markers to differentiate histological types of cancer histology. *Clin Radiol* 2018;73:1033–40.
- Zhang Z, Zou H, Yuan A, et al. A single enhanced dual-energy CT scan may distinguish lung squamous cell carcinoma from adenocarcinoma during the venous phase. *Acad Radiol* 2020;27:624–9.
- Cheng SM, Ling W, Zhu J, et al. Dual energy spectral CT imaging in the assessment of gastric cancer and cell proliferation: a preliminary study. *Sci Rep* 2018;8:17619.